

# Shaking table test study on a steel frame with autoclaved aerated concrete walls

Caiyuan Cheng | Liusheng He

Research Institute of Structural Engineering and Disaster Reduction, Tongji University, Shanghai, China

## Correspondence

Dr. Liusheng He, Research Institute of Structural Engineering and Disaster Reduction, Tongji University, 1239 Siping Road, Shanghai 20092, China.

Email: hls@tongji.edu.cn

## Funding information

National Key Research and Development Plan of China, Grant/Award Number: 2017YFC1500701

## Abstract

This paper studies the seismic performance of a steel frame with autoclaved aerated concrete (AAC) walls through full-scale shaking table tests. In the tested single-span two-storey steel frame, two types of AAC walls, AAC panel, and AAC block masonry wall, were adopted. Damage distribution and progress, acceleration and displacement responses, and the effect of window openings and corresponding strengthening methods were investigated. Test results showed that good seismic performance of the model structure was achieved with using both types of AAC walls, the connection used between AAC walls and steel structure was reliable and the reinforcement applied for the wall near window openings was found effective.

## KEYWORDS

autoclaved aerated concrete wall, block masonry wall, connection, seismic performance, shaking table test

## 1 | INTRODUCTION

Due to the advantage of steel, such as high strength, light weight, excellent seismic performance, and quick construction, steel structures are widely used in civil and industrial buildings. However, the development of infill walls for steel structures are lacking behind. It is preferred that the infill walls with light weight, are suitable for industrial mass production, and have good workability. Autoclaved aerated concrete (AAC) wall is such a kind, which is high in strength but light in weight, soundproof, exceptional in thermal insulation, suitable for mass production in the factory, and convenient for on-site installation. Considerable amount of research on AAC walls have been conducted, with the focus on primary material property [1], reinforcement [2–4], thermal behavior [5,6], mechanical behavior [7,8], etc. However, the seismic performance of AAC walls in full-scale or large-scale structure has less been studied.

To study the seismic performance of AAC walls installed in steel structures, full-scale shaking table tests were conducted on a steel structure with two types of AAC walls. The objectives of this study are to study: (1) the seismic performance of the steel structure with AAC walls; (2) damage progress; (3) performance of the connection between the AAC wall and steel structure; and (4) the effect of openings in AAC walls.

## 2 | PREPARATION OF TESTS

### 2.1 | Test specimens

Full-scale shaking table tests on a single-span two-storey steel frame structure were conducted. The floor-plan size of the steel structure was  $3.1 \times 4$  m (as shown in Figure 1a) and the storey height was 2.9 m. The steel frame was built with H-shaped structural steel, H150  $\times$  150  $\times$  8  $\times$  8 for columns and H180  $\times$  100  $\times$  6  $\times$  8 for beams. The steel grade was Q235B in the Chinese standard. The slab was the profiled sheet-concrete composite floor with a thickness of 130 mm and the concrete used was C30.

For comparison, both AAC panels and block masonry walls were used in the model structure. AAC panels with unit dimensions of 2,900  $\times$  600  $\times$  150 mm were installed along the long side of the floor plan (X direction), as shown in Figure 1b. The pipe anchors were used at both top and bottom ends of each panel in connection to the steel structure. A schematic diagram of the pipe anchor is shown in Figure 2. The joining bands between the side-by-side placed AAC panels were strengthened with glued grid cloth, to improve the whole wall's integrity. After all AAC panels were placed, the exterior surface of the whole wall was smoothed with paint filler.

# Flexural strength of AAC masonry with bed joint reinforcement

Adam Piekarczyk

Department of Building Structures, Silesian University of Technology, Akademicka 5, 44-100 Gliwice, Poland

## Correspondence

Dr. Adam Piekarczyk, Department of Building Structures, Silesian University of Technology, Akademicka 5, 44-100 Gliwice, Poland.  
Email: adam.piekarczyk@polsl.pl

## Abstract

The paper presents the results of comparative investigations of flexural strength of unreinforced and reinforced autoclaved aerated concrete (AAC) masonry. The plane of masonry failure was perpendicular to the bed joints plane. Reinforcement in the form of steel wire, glass, and basalt fibers placed in masonry bed joints influenced the higher flexural strength and crack resistance of masonry specimens. Reinforced masonry showed plastic nature after cracking allowing for large horizontal displacements and transferring the substantial loads perpendicular to the surface of masonry in relation to the unreinforced masonry. For most reinforced masonry specimens, the strengthening after cracking was observed which means that the maximum value of load occurred in the cracked masonry.

## KEYWORDS

AAC masonry units, bed joint reinforcement, flexural strength

## 1 | THE FAILURE MECHANISM AND FLEXURAL STRENGTH OF MASONRY

Depending on the orientation of the plane perpendicular to the wall plane, in which the bending moment acts on the wall, according to EN 1996-1-1 [1], two cases occur. In the first one, the masonry failure takes place in a plane parallel to the bed joints, and due to the adhesion between the masonry units and the mortar usually lower than the tensile strength of masonry units, the plane of failure occurs in most cases through the masonry bed joints. The characteristic flexural strength of masonry is then designated as  $f_{xk1}$ . In the second case, failure of masonry occurs in a plane perpendicular to the bed joints. Failure of the masonry in this case may consist of, in exceeding, the flexural strength of masonry units, when the plane of failure passes through masonry units and vertical head joints. This way of failure often occurs when the head joints are unfilled (Figure 1a) or a "stepped" crack may appear along the bed and head joints when the decisive failure factor is primarily the ultimate torsional shear stress in the bed joint (Figure 1b). The mixed mechanism of failure is also possible. In this situation, the flexural strength, according to EN 1996-1-1 [1] standard is marked with the symbol  $f_{xk2}$ .

Increasing the flexural load capacity of the masonry when the plane of failure is perpendicular to the bed joints is possible due to the reinforcement placed in the bed joints. The EN 1996-1-1 [1] introduces the concept of the design apparent strength  $f_{xd2,app}$ , which is determined by comparing the design resistance of the unreinforced wall section

with the strength  $f_{xd2,app}$  with the design resistance of the reinforced masonry section. This paper presents the results of the tests of the influence of the meshes of various materials placed in the masonry bed joints on flexural strength when the plane of failure is perpendicular to the bed joints, and effect of this type of reinforcement on the load causing masonry cracking. During the tests, the horizontal displacement (deflection) of masonry specimens was also measured.

## 2 | MATERIALS AND SPECIMENS

### 2.1 | Materials

Walls were made of autoclaved aerated concrete (AAC) blocks SOL-BET Optimal P+W with a mean declared density equal to  $600 \text{ kg/m}^3$  with tongue and groove. The declared width of the blocks was  $180 \pm 1.5 \text{ mm}$ , height  $240 \pm 1.0 \text{ mm}$  and length  $590 \pm 1.5 \text{ mm}$ . Blocks belonged to category I of masonry units. The mean declared normalized compressive strength of the blocks was not less than  $4.0 \text{ N/mm}^2$ . According to the results of tests carried out at the Department of Building Structures of the Silesian University of Technology [2], the mean normalized compressive strength  $f_b$  determined according to EN 772-1 standard [3] on cubic samples with a side  $100 \text{ mm}$  cut from whole blocks was equal to  $4.04 \text{ N/mm}^2$  ( $f_b = 5.05 \text{ N/mm}^2$ ,  $s = 0.341 \text{ N/mm}^2$ ,  $\nu = 6.76\%$ ) with the load perpendicular to the bed face, where  $f_b$  is the mean strength,  $s$  is the standard deviation

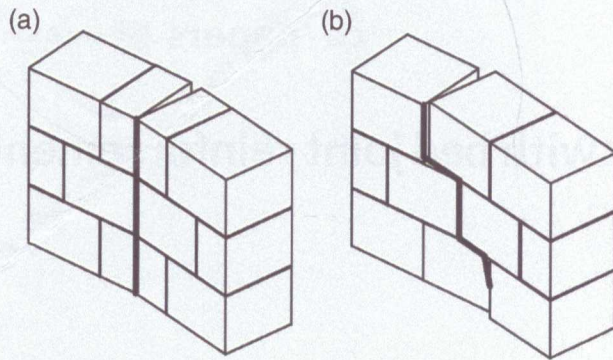


**FIGURE 1** Flexural failure of masonry in the plane perpendicular to the bed joints when the failure plane running through: (a) masonry units and head joints, (b) bed and vertical joints

and  $\nu$  is the coefficient of variation. In the case of a load perpendicular to the head face, the normalized mean compressive strength was equal to  $4.10 \text{ N/mm}^2$  ( $f_B = 5.13 \text{ N/mm}^2$ ,  $s = 0.395 \text{ N/mm}^2$ ,  $\nu = 7.71\%$ ) just as mean normalized strength in the direction perpendicular to the stretcher face ( $f_B = 5.13 \text{ N/mm}^2$ ,  $s = 0.327 \text{ N/mm}^2$ ,  $\nu = 6.38\%$ ). The mean strength of whole blocks (determined on six masonry units) was equal to  $3.65 \text{ N/mm}^2$  ( $s = 0.363 \text{ N/mm}^2$ ,  $\nu = 9.95\%$ ), while the mean strength determined of four cylinders of diameter 55 mm and height of 120 mm cut out of blocks was  $4.14 \text{ N/mm}^2$  ( $s = 0.109 \text{ N/mm}^2$ ,  $\nu = 2.64\%$ ).

The specimens were made using system mortar for thin joints SOL-BET 01 class M5. According to the tests [2] carried out according to EN 1015-11 standard [4], mean flexural strength was equal to  $2.0 \text{ N/mm}^2$  ( $s = 0.060 \text{ N/mm}^2$ ,  $\nu = 3.0\%$ ) and mean compressive strength of  $6.1 \text{ N/mm}^2$  ( $s = 0.374 \text{ N/mm}^2$ ,  $\nu = 6.13\%$ ).

The reinforcement applied in the masonry bed joints were of three types:

1. Welded steel mesh with  $12.7 \times 12.7 \text{ mm}$  square mesh and 1.05 mm wire diameter (Figure 2a). The mesh was protected against corrosion with a layer of zinc in an amount not less than  $350 \text{ g/m}^2$ . The tensile strength of a single wire, as declared by the manufacturer, was 350 N.
2. Glass fibre mesh with  $9 \times 13 \text{ mm}$  mesh, the impregnated mesh grammage  $335 \pm 30 \text{ g/m}^2$  (Figure 2b). The declared tensile strength of the 5 cm wide mesh strip was not less than 4000 N along the

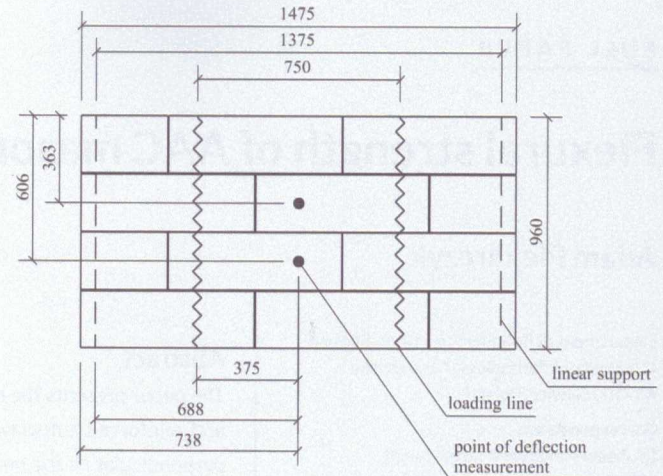


**FIGURE 3** Masonry specimens used in tests according to EN 1052-2 standard [5]

warp and not less than 3000 N in the direction of weft. The tensile strength of a single weave along the weft was estimated at 715 N. According to the manufacturer's declaration, the mesh was resistant to alkali and putrefaction.

3. Basalt fibre mesh with  $30 \times 30 \text{ mm}$  mesh and  $260 \pm 10 \text{ g/m}^2$  grammage (Figure 2c). The declared tensile strength of the mesh along warp and weft was the same and was not less than 50,000 N/m. The tensile strength of the single weave was not less than 1250 N. The bulk density of the basalt fibers was equal to  $2.67 \pm 5\% \text{ g/cm}^3$ . The declared melting temperature was  $1350 \pm 100^\circ\text{C}$ .

## 2.2 | Specimens

The shape and overall dimensions of the masonry specimens for test of flexural strength when the plane of failure is perpendicular to the bed joints were made in accordance with the requirements of EN 1052-2 [5] standard. Figure 3 shows the nominal dimensions of the specimen used in tests. Dimensions were determined assuming the nominal dimensions of masonry units and thin bed joints and head joints thickness equal to 3 mm. The standard test method is often called the method of four load points. The specimens are supported freely along two linear supports spaced about 50 mm from the vertical edges of the masonry (dashed lines in Figure 3). The load also acts

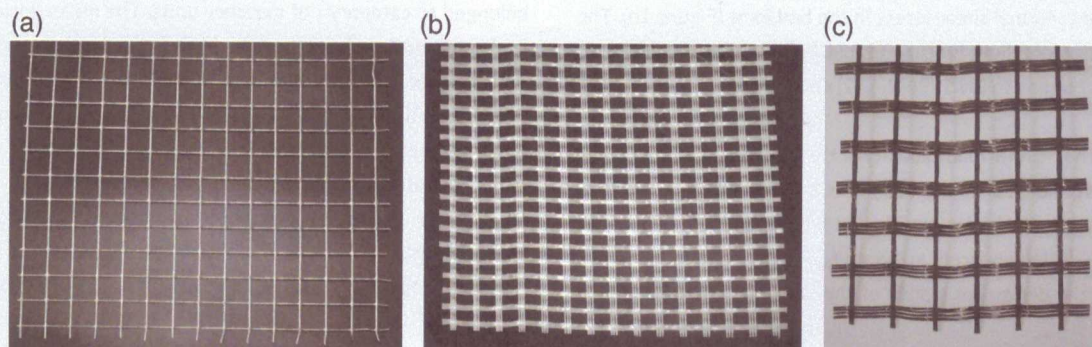


**FIGURE 2** Meshes used as reinforcement placed in masonry bed joints made of: (a) steel wire, (b) glass fibers, (c) basalt fibers

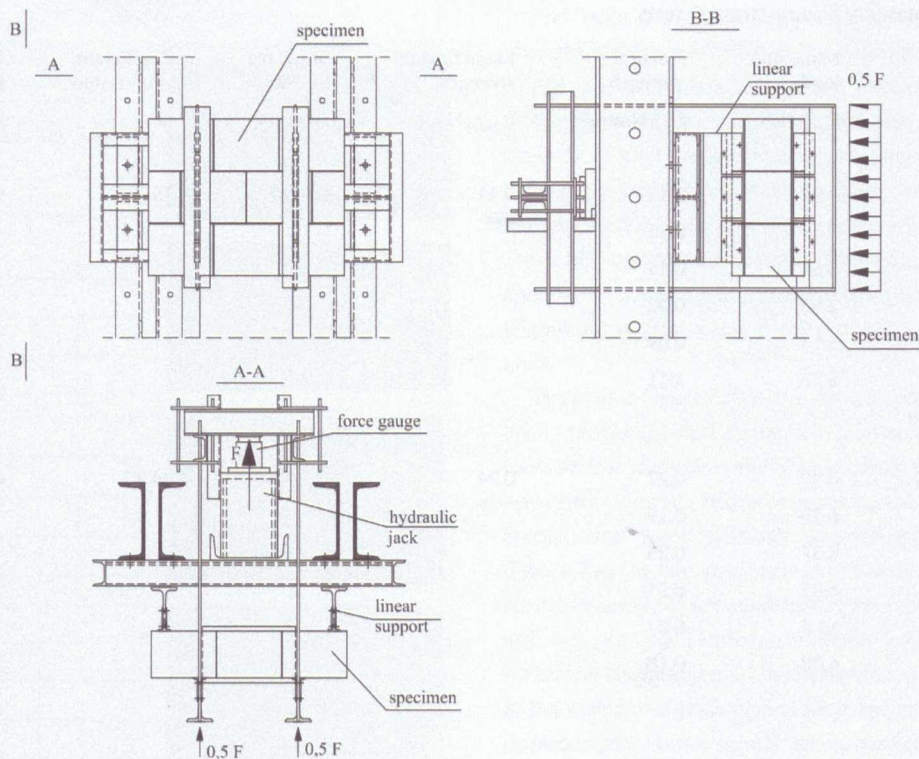


FIGURE 4 Scheme of stand for testing the flexural strength of masonry when plane of failure is perpendicular to the bed joints



FIGURE 5 Specimen in test stand

along two lines (wavy lines in Figure 3) at the same distance from the supports, so that at least one vertical head joint is between the load lines. In case of described investigations, the distance between the support lines was  $l_1 = 1375$  mm, while the distance between the load lines was  $l_2 = 750$  mm, thus the ratio  $l_2/l_1$  ranged from 0.4 to 0.6 required in the standard [5].

In total, 24 specimens were tested: six unreinforced masonry and six reinforced specimens with each type of reinforcing meshes. Reinforcement was placed in each of three bed joints. The reinforcement was continuous over the length of each joint. In the cross-section of the single bed joint there were 13 steel wires or 12 weaves of glass fibers or six weaves of basalt fibers. The effective width of used steel wire mesh was equal to 152 mm, width of glass fibers mesh was equal

TABLE 1 Values of  $k$  coefficient

$n$	6	7	8	9	10
$k$	2.18	2.08	2.01	1.96	1.92

to 143 mm, in case of basalt fibers effective width was 150 mm. The unreinforced specimens were marked with X2N- $i$ , specimens with steel wire meshes were designated X2S- $i$ , the specimens reinforced with glass fibers meshes had the designation X2G- $i$  and the specimens with basalt fibers reinforcement had X2B- $i$  symbols, where  $i = 1, 2, \dots, six$  were the number of the specimen in a given test series.

### 3 | TEST STAND AND TESTING PROCEDURE

The tests were carried out in a specially designated steel test stand meeting the requirements of EN 1052-2 [5] standard, the sketch of the test stand is shown in Figure 4 and photograph in Figure 5. Linear supports and elements for direct linear loading of the specimens were constructed from several parts to ensure uniform load distribution. These elements were hinged to the members transferring the total load.

The specimens were tested in a vertical position to avoid the impact of the self-weight of masonry on the calculated value of stresses in the bent section.

In addition to measuring the force  $F$ , the horizontal displacements (deflections) were also measured at two points in the middle of the span between supports lines in the two inner layers of the specimen (see Figure 3). Displacement transducers with the range up to 20 mm were in contact with the compressed face of the bent specimen.

TABLE 2 Results of masonry flexural strength tests

Specimen	Maximum load $F_{i,max}$ , kN	Flexural strength $f_{x2,i}$ , N/mm <sup>2</sup>	Mean flexural strength $f_{x2,mv}$ , N/mm <sup>2</sup>	Standard deviation $s$ , N/mm <sup>2</sup>	Coefficient of variation %	Characteristic flexural strength $f_{xk2}$ , N/mm <sup>2</sup>
<b>Unreinforced masonry</b>						
X2N-1	4.29	0.13	0.11	0.0167	15.7	0.07
X2N-2	3.68	0.11				
X2N-3	3.69	0.11				
X2N-4	2.68	0.08				
X2N-5	3.14	0.09				
X2N-6	3.73	0.11				
<b>Masonry with steel wire reinforcement</b>						
X2S-1	8.93	0.27	0.24	0.0598	24.8	0.14
X2S-2	6.39	0.19				
X2S-3	8.37	0.25				
X2S-4	6.85	0.21				
X2S-5	11.3	0.34				
X2S-6	6.08	0.18				
<b>Masonry with glass fibers mesh reinforcement</b>						
X2G-1	8.93	0.27	0.25	0.0296	11.8	0.19
X2G-1	7.05	0.21				
X2G-1	7.97	0.24				
X2G-1	9.92	0.30				
X2G-1	8.06	0.24				
X2G-1	9.07	0.24				
<b>Masonry with basalt fibers mesh reinforcement</b>						
X2B-1	10.2	0.31	0.259	0.0303	11.7	0.20
X2B-2	8.61	0.26				
X2B-3	7.75	0.23				
X2B-4	8.99	0.27				
X2B-5	8.76	0.26				
X2B-6	7.30	0.22				

#### 4 | TEST RESULTS

According to the standard EN 1052-2 [5], the flexural strength for each specimen should be determined with an accuracy of 0.01 N/mm<sup>2</sup> from the formula

$$f_{xi} = \frac{3F_{i,max}(l_1 - l_2)}{2bt_u^2}, \quad (1)$$

where  $F_{i,max}$  is the maximum value of obtained force (ultimate load),  $l_1$  is the spacing of supports,  $l_2$  is the spacing of load lines,  $b$  is the width of the specimen,  $t_u$  is the specimen thickness, usually equal to the thickness of masonry.

The mean value  $f_{x,mv}$  and the characteristic value  $f_{xk}$  of flexural strength are also determined with an accuracy of 0.01 N/mm<sup>2</sup>. The characteristic strength in case when more than five specimens of a

given type have been tested, as in the described tests, is calculated using the following formulas:

$$y_i = \log 10 f_{xi}, \quad i = 1, 2, \dots, n \quad (2)$$

$$y_{mv} = \frac{\sum_{i=1}^n y_i}{n} \quad (3)$$

$$y_c = y_{mv} - ks \quad (4)$$

$$f_{xk} = 10^{y_c} \quad (5)$$

where  $n$  is the number of tested specimens,  $s$  is the standard deviation of the set of values  $\{y_i\}$ ,  $k$  is coefficient dependent on the number of specimens according to Table 1.

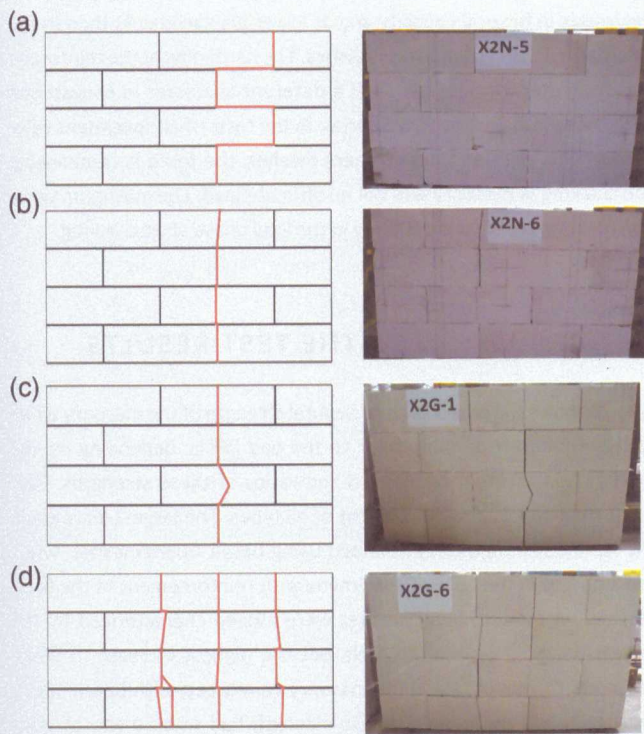


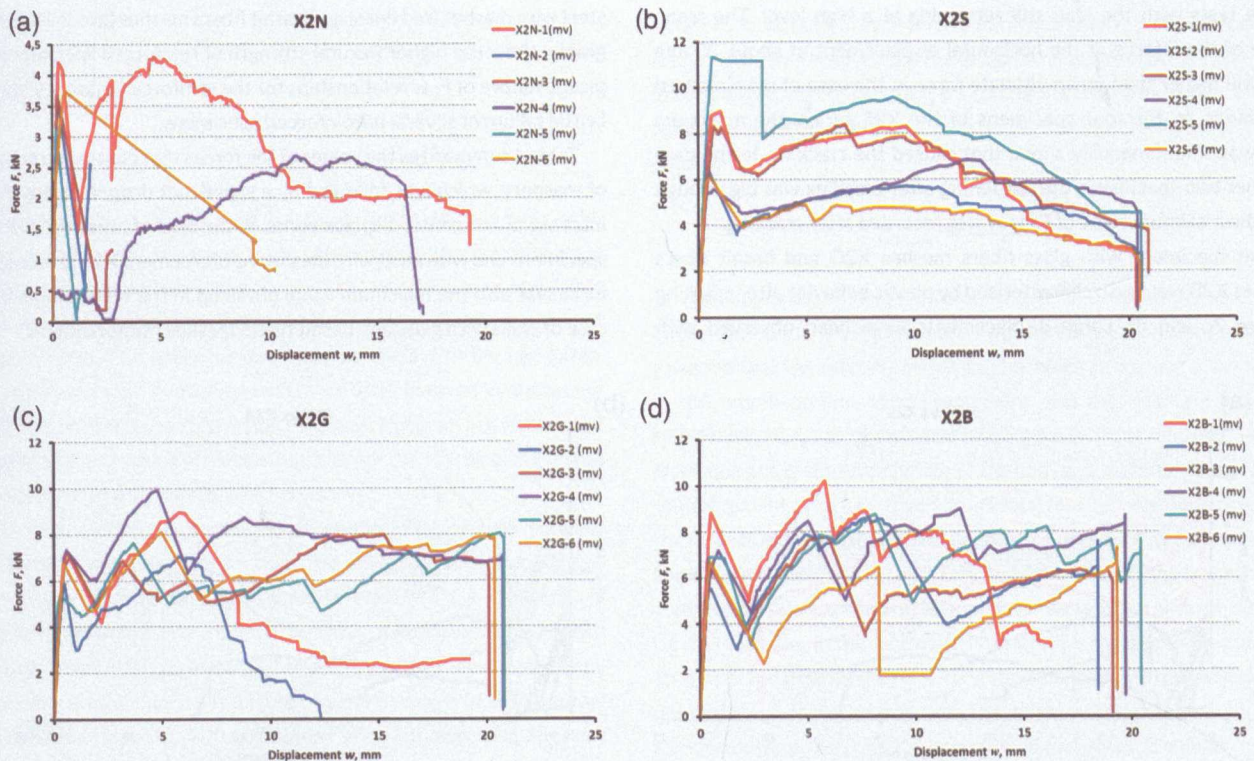
**FIGURE 6** Flexural failure of masonry specimens with cracks passing through: (a) head and bed joints of masonry without reinforcement, (b) head joints and masonry units in unreinforced specimen, (c) head joints and masonry units in one plane of failure of masonry with reinforcement, and (d) in many planes of failure of reinforced masonry

The Table 2 presents the results of tests of masonry flexural strength at the plane of failure perpendicular to the bed joints.

Figure 6 presents drawings and photos showing the failure of selected specimen's characteristic for each tested series. In case of majority of specimens without reinforcement cracks running only through the bed joints and unfilled bed joints (Figure 6a), except for one specimen X2N-6 where the vertical plane of failure passed through the head joints and masonry units (Figure 6b). The failure of reinforced specimens consisted in the creation of a single (Figure 6c) or multiple (Figure 6d) vertical cracks running through head joints and masonry units.

The plots in Figure 7 show the dependences of mean values of specimen's horizontal displacements in relation to  $F$  force. In the case of four specimens without reinforcement from the X2N series, the failure was brittle, meaning that after reaching the maximum load, masonry cracked and force suddenly dropped with small displacements (Figure 7a). The two specimens in this series, however, show specific plastic behavior, which consisted in the fact that after cracking, the wall was able to transfer a relatively large force with significant horizontal displacements. The maximum load value was obtained not at the moment of cracking, but after hardening the masonry at high displacements. Such a specific mechanism of failure could have been caused by shape of the face of masonry units equipped with tongue and groove and wedging of the blocks in their mutual rotation.

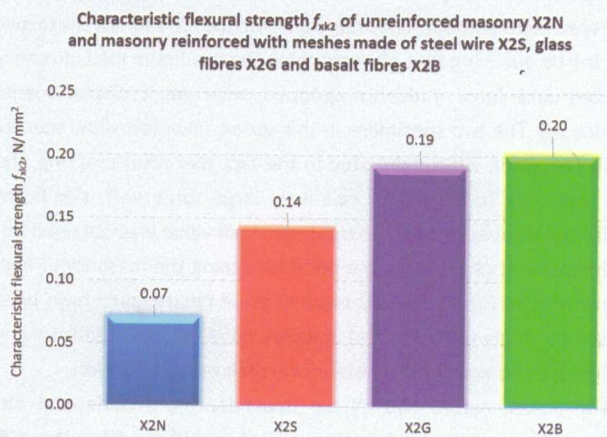
The plastic nature had all the dependences of horizontal displacements from the load in the case of specimens from the X2S series (Figure 7b), i.e. containing steel meshes in the bed joints. After cracking, very large displacements of the masonry were obtained



**FIGURE 7** The dependences of the horizontal displacements  $w$  of the specimens from the  $F$  force in case of the masonry: (a) without reinforcement, (b) with steel wire meshes, (c) with glass fibers meshes, (d) with basalt fibers meshes

**TABLE 3** Characteristic flexural strength of unreinforced masonry and masonry with various reinforcement

Specimens	Characteristic flexural strength $f_{xk2}$ , N/mm <sup>2</sup>	$f_{xk2,(S,G,B)}/f_{xk2,N}$ Ratio
X2N - unreinforced	0.07	1.00
X2S - steel wire mesh reinforcement	0.14	2.00
X2G - glass fibers mesh reinforcement	0.19	2.70
X2B - basalt fibers mesh reinforcement	0.20	2.86

**FIGURE 8** Comparison of unreinforced and reinforced masonry flexural strength  $f_{xk2}$ 

in the tests with the load still remaining at a high level. The mean value of the  $F$  force at the horizontal displacement of about 20 mm was still higher than mean ultimate force in the case of unreinforced specimens. In the four specimens of the X2S series, the maximum load was simultaneously a load that caused the cracking. In the case of other two specimens, the hardening after cracking was big enough that the maximum value of  $F$  force was recorded after cracking.

The specimens with glass fibers meshes X2G and basalt fibers meshes X2B were also characterized by plastic behavior after cracking (Figure 7c and d). Large displacements have been observed with

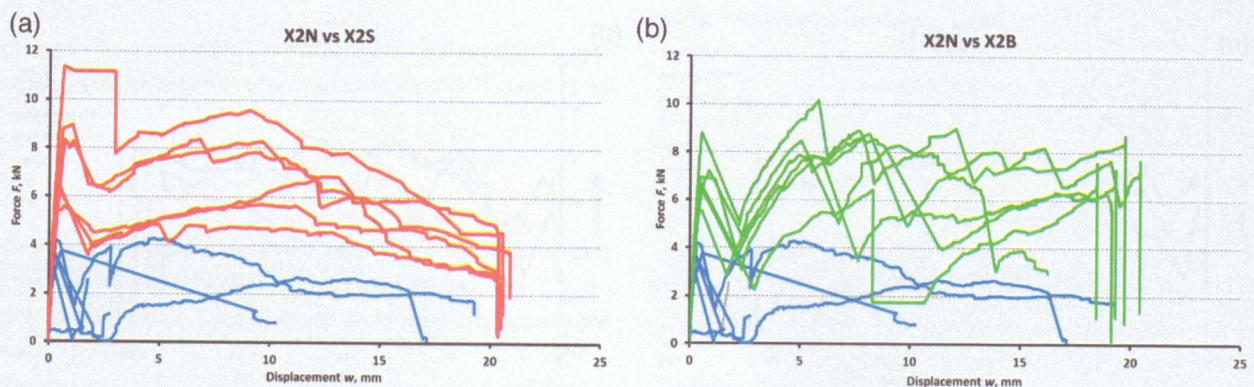
relatively high loads. In a few cases, however, there were much greater decreases in flexural capacity and at lower displacements than in the masonry reinforced with steel meshes. The hardening of the reinforced masonry after cracking also had a different character in comparison with the specimens form X2S series. In the tests of all specimens reinforced with glass and basalt fibers meshes, the force accompanying the cracking of masonry was not an ultimate load. The maximum value of  $F$  forces were always obtained in the load phase after cracking.

## 5 | DISCUSSION OF THE TEST RESULTS

Table 3 shows the characteristic flexural strength of the masonry when plane of failure  $\perp$  perpendicular to the bed joints, depending on the type of reinforcing meshes used and ratios of these strengths. Visible is the impact of reinforcement of all types. The largest increase in the flexural strength was obtained using basalt fibers meshes, while the smallest in the case of specimens with reinforcement in the form of steel wire mesh. Steel meshes were indeed characterized by the lowest declared tensile strength, but the highest increase in flexural strength was obtained for masonry reinforced with basalt fibers meshes, while the largest tensile strength had mesh made of glass fibers. The increase in flexural strength was therefore not proportional to the tensile strength of the applied reinforcement. Figure 8 shows a graphical comparison of the characteristic masonry flexural strength  $f_{xk2}$ .

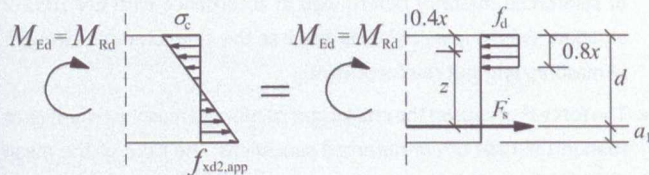
Figure 9 shows the comparison of the relationships between the horizontal displacements  $w$  and force  $F$  that causes bending of masonry for unreinforced masonry (blue lines) and reinforced masonry with steel wire meshes (red lines) and basalt fibers meshes (green lines). The graphs show the higher flexural strength of reinforced specimens and plastic nature of  $F$ - $w$  relationships for the reinforced masonry and the brittle failure of several unreinforced specimens.

Table 4 summarizes the values of the forces that causes the cracking of masonry, which was followed by a significant drop in strength and increase of horizontal displacements. In the case of unreinforced X2N specimens and with steel wire meshes reinforcement X2S, the cracking force was also the maximum value obtained in the tests, unlike in the case of walls with glass and basalt fibers meshes reinforcement.

**FIGURE 9** Comparison of dependences the horizontal displacements  $w$  from the  $F$  force obtained for unreinforced specimens (blue lines) and reinforced specimens with: (a) steel wire meshes (red lines), (b) basalt fibre meshes (green lines)

**TABLE 4** Comparison of forces at the moment of masonry cracking

Specimens	Mean cracking force $F_{cr,mv}$ , kN	Standard deviation $s_{Fcr}$ , kN	Coefficient of variation $v_{Fcr}$ , %	$F_{cr,mv(S,G,B)}/F_{cr,mv,N}$ ratio
X2N - unreinforced	3.69	0.38	10.2	1.00
X2S - steel wire mesh reinforcement	7.78	2.19	28.2	2.11
X2G - glass fibers mesh reinforcement	6.63	0.82	12.4	1.80
X2B - basalt fibers mesh reinforcement	6.93	1.08	15.6	1.88



**FIGURE 10** Method of determination of apparent flexural strength  $f_{xk2,app}$

**TABLE 5** Comparison of bending moments obtained from the tests and calculations

Specimens	Bending moment from the tests	Calculated bending moment	$M_{cal}/M_{obs}$ ratio
	$M_{obs}$ , kNm	$M_{cal}$ , kNm	
X2N - unreinforced	0.55	-	-
X2S - steel wire mesh reinforcement	1.25	0.834	0.67
X2G - glass fibers mesh reinforcement	1.30	1.55	1.19
X2B - basalt fibers mesh reinforcement	1.34	1.42	1.06

The comparison of the mean cracking forces obtained for reinforced masonry and the mean force causes cracking of unreinforced specimens (sixth column in the Table 4) shows that use of bed joints reinforcement significantly increases the cracking resistance of bent masonry when the plane of failure is perpendicular to the bed joints. The largest increase in cracking resistance was observed in the case of specimens reinforced with steel wire meshes, although in this case, the variation of the cracking force was much larger than in the other tested series of reinforced masonry specimens.

The characteristic flexural strength of unreinforced walls equal to  $0.07 \text{ N/mm}^2$  was much lower than the characteristic strength  $f_{xk2}$  given in the table in paragraph 3.6.3 of EN 1996-1-1 [1] standard equal to  $0.30 \text{ N/mm}^2$  and slightly lower than value given in the Polish National Annex equal to  $0.025 f_b$  for masonry with unfilled head joints, which with average normalized compressive strength of blocks equal to  $4.04 \text{ N/mm}^2$  gives  $f_{xk2} = 0.101 \text{ N/mm}^2$ . This situation also does not refer to note 4 in paragraph 3.6.3(3) of EN 1996-1-1 [1], which states that the strength  $f_{xk2}$  should not be greater than flexural strength of masonry units, because in the case of five out of six of the tested

unreinforced specimens, the plane of failure ran through the bed and unfilled head joints, not through the masonry units.

Paragraph 6.6.2(9) of EN 1996-1-1 [1] introduces the concept of apparent flexural strength  $f_{xk2,app}$  of a reinforced masonry with reinforcement in bed joints when the plane of failure is perpendicular to the bed joints. Apparent strength is determined by comparing the design flexural strength of reinforced wall with the flexural strength of unreinforced wall with tensile strength equal to  $f_{xk2,app}$  and with the same thickness (Figure 10).

The load capacity for bending of unreinforced masonry is assumed to be equal

$$M_{Rd} = f_{xd2,app} Z = f_{xd2,app} \frac{t^2}{6}, \quad (6)$$

where  $Z$  is the elastic bending section modulus per unit wall height,  $t$  is the wall thickness. The load capacity for bending for the reinforced masonry can be calculated from the formula

$$M_{Rd} = F_s z = A_s f_{yd} z, \quad (7)$$

where  $A_s$  is the total area of tensile reinforcement in bed joints per one meter of the wall height,  $f_{yd}$  is the design strength of steel,  $z$  is lever arm in bending section of masonry. By comparing the formulas (6) and (7), the value of the apparent flexural strength can be determined from the equation

$$f_{xd2,app} = \frac{6A_s f_{yd} z}{t^2}. \quad (8)$$

This approach is correct when the tensile reinforcement used in the bed joints is concentrated in the cross-section and it can be assumed that the ultimate stress ( $f_{yd}$  for steel) occurs simultaneously in the whole section of reinforcement and the resultant force in reinforcement  $F_s$  can be assumed (see Figure 8). If the reinforcement is distributed over the entire width of the bed joint, as in the case of mesh reinforcement, with a relatively small total tensile force occurring in all the strands of the mesh, the balancing force present in the compressed zone of masonry is small, and hence small there is also the height of the compression zone  $x$ , which in turn leads to the fact that all mesh strands can be in tension. In the case when limit stress is reached in the outmost strands of the mesh in the remaining strands stress will decrease to values close to 0 at the neutral axis. The height of the compression zone  $x$  can be determined from the condition of forces static equilibrium

$$0.8fbx = \sum_{i=1}^{n_l} F_{ti}, \quad (9)$$



where  $f$  is the compressive strength of the masonry in the direction parallel to the bed joints,  $b$  is the width of the calculated section,  $F_{ti}$  is the tensile force in the individual strand of the mesh,  $n$  is the number of the strand in tension. The bending capacity of such section  $M_R$  can be determined, e.g., from the moment equation against the center of the masonry compression zone from the equation

$$M_R = \sum_{i=1}^{n_i} F_{ti} (h - 0.4x - a_1 - (i - 1)s), \quad (10)$$

where  $a_1$  is the distance of the most tensioned strand from the edge of the cross-section,  $s$  is the distance between the strands of the mesh. At the condition that

$$(n_i - 1)s \leq h - x - a_1, \quad (11)$$

The problem is therefore the correct determination of tensile forces  $F_{ti}$  occurring in individual strands of the mesh and knowledge of the compressive strength of the masonry  $n$  the direction parallel to the bed joints. In order to correctly determine the values of  $F_{ti}$  forces, it is necessary to know design limit value of the  $F_t$ , which in the case of steel reinforcement corresponds to the force occurring in the reinforcement reaching yielding point  $f_y$ , the strain  $\epsilon_y$  corresponding to the  $F_t$  force (or modulus of elasticity) and the ultimate permissible strain in reinforcement  $\epsilon_u$ . It is also necessary to determine the design relationship tensile force-strains (bilinear relation with the horizontal or inclined upper branch of the graph or other).

Unfortunately, at the time of elaborating this paper, the above mentioned parameters of the applied reinforcement were not known. Only the declared tensile strength of meshes was available. On this basis, however, an attempt was made to roughly estimate the bending capacity of the reinforced masonry using formulas (9)–(11). It was assumed, with the awareness of the error made, that in the most tensile weave, the maximum tensile force reach value calculated on the basis of the declared tensile strength of the mesh and in subsequent weaves these forces decrease linearly depending on the distance from the neutral axis. In this way, the values of  $M_{cal}$  bending moment was calculated, which are shown in Table 5 and compared with the maximum bending moments obtained in the tests  $M_{obs}$ . In the case of masonry with reinforcement made of steel wire, the value of the moment calculated was less than that obtained in the tests, whereas in case of specimens reinforced with glass and basalt fibers meshes, the calculated moments were greater than the ones obtained in the tests, but quite close to them, and this outcome taking into account rough estimation of bending moment capacity can be considered a good result.

## 6 | CONCLUSIONS

The results of flexural strength tests of thin bed joints and unfilled head joints unreinforced masonry and masonry with reinforcement in form of the meshes made of various materials placed in bed joints with the plane of failure perpendicular to the masonry bed joints carried out in previously described range allow to state that:

- Flexural strength of masonry with reinforcement is much higher than that of unreinforced masonry; characteristic flexural strength of reinforced masonry determined in accordance with EN 1052-2 standard was at least twice as great as the characteristic strength of masonry without reinforcement.
- The force that caused the cracking of reinforced masonry was higher than in the case of unreinforced specimens; the ratio of the mean cracking force obtained in the tests of reinforced specimens to the mean cracking force for unreinforced masonry was not less than 1.80.
- The maximum horizontal displacement (deflection) of reinforced bending masonry was greater than in the case of unreinforced masonry; the use of bed joint reinforcement allowed to carry a relatively high load after the occurrence of cracks at large horizontal displacements; in the case of majority of reinforced specimens, maximum loads were obtained in the phase of masonry hardening after cracking with exception of several specimens reinforced with steel wire meshes.

## REFERENCES

1. EN 1996-1-1. Eurocode 6. Design of masonry structures. Part 1-1: General rules for reinforced and unreinforced masonry structures.
2. Łukasz D, Radosław J. Wpływ rodzaju zaprawy na parametry mechaniczne murów z ABK poddanych ścisnaniu (Influence of the kind of mortar on mechanical parameters of AAC masonry subjected to compression). *Materiały Budowlane*. 2015;512(4):3–7.
3. EN 772-1. Methods of test for masonry units. Part 1: Determination of compressive strength.
4. EN 1015-11. Methods of test for mortar for masonry. Part 11: Determination of flexural and compressive strength of hardened mortar.
5. EN 1052-2. Methods of test for masonry. Part 2: Determination of flexural strength.

**How to cite this article:** Piekarczyk A. Flexural strength of AAC masonry with bed joint reinforcement. *ce papers*. 2018;2:389–396. <https://doi.org/10.1002/cepa.887>